

# Dispersion of Lamb Waves Propagating Under a Periodic Metal Grating in AlN Plates

Natalya Naumenko

National University of Science and Technology "MISIS", Moscow, Russian Federation

**Abstract** — Dispersion of Lamb waves propagating in AlN plates with a periodic Al grating on the top surface and an Al electrode on the bottom surface is investigated using the numerical technique SDA-FEM-SDA. The structures of typical Lamb waves are examined via visualization of the instantaneous displacement fields in the AlN plate. The mechanism of building hybrid modes, which arise from intermode coupling between the counter-propagating Lamb waves of different symmetry and order, is illustrated by the mode propagating with wavelength  $\lambda=3p$ , where  $p$  is the pitch of the grating.

(SAW) dispersion because Lamb waves are guided in a plate of a finite thickness and their structure strongly depends on the thickness in wavelengths. This paper is aimed at numerical investigation of Lamb wave dispersion in AlN thin plates with a periodic Al grating on top and a uniform Al electrode of finite thickness at the bottom. Of particular interest are propagation of higher-order Lamb waves in the grating and interactions between Lamb waves, which occur when a wavelength in the grating differs from  $\lambda_0=2p$ .

## I. INTRODUCTION

Lamb wave resonators employing aluminum nitride (AlN) thin plates or membranes appear to be an attractive new type of device for wireless communication systems, sensors and other high-frequency applications. In resonators, Lamb waves are normally excited by interdigital transducers (IDTs) and reflected by electrodes of a periodic metal grating and resonator edges. In high-symmetry materials, such as AlN, the dispersion of Lamb waves, which is usually understood as a velocity dependence on plate thickness-to-wavelength ratio, can be predicted fairly accurately using simple equations [1]. The influence of a periodic grating and metallization of an AlN bottom surface can be simulated by means of well-known numerical techniques [2-4]. However, the behavior of Lamb waves under periodic metal structure is not yet well understood.

Most of the reported Lamb wave characteristics in AlN refer to zero-order modes  $s_0$  and  $a_0$ . Higher-order Lamb waves, the number of which increases with plate thickness, look more attractive for high-frequency applications due to higher propagation velocities, but their characteristics are more sensitive to the plate thickness and the geometrical parameters of the grating. Therefore, improved models are required for accurate simulation of resonators employing these modes. Another aspect of particular interest is the influence of detuning from the Bragg's reflection condition in Lamb wave resonators, expressed as  $\lambda_0=2p$  where  $p$  is the pitch of the grating, on the resonator performance. The finite length of a resonator means that a set of waves with wavelengths varying in a range  $\lambda_0\pm\Delta$  can be efficiently reflected by the grating. It is apparent that a simulation of Lamb wave resonators must consider the variation of Lamb wave characteristics with spectral frequency  $s=p/\lambda$ .

In general, the dispersion of Lamb waves in a periodic grating is more complicated than surface acoustic wave

## II. METHOD OF INVESTIGATION

Characteristics of Lamb waves, which propagate in a piezoelectric plate under a periodic metal grating, were calculated via numerical solution of equation  $Y(f,s)^{-1}=0$  (SC condition) or  $Y(f,s)=0$  (OC condition) where harmonic admittance of the grating  $Y$  is a function of frequency  $f$  and normalized wave number (spectral frequency)  $s=k/2k_0$ , and  $k_0=\pi/p$  is the unperturbed wave number. Numerical functions  $Y(f,s)$  were simulated with the universal software SDA-FEM-SDA [5], which enables analysis of different types of acoustic waves, including Lamb waves, and considers the geometrical parameters of Lamb wave resonators: the thicknesses of a plate and electrodes of the grating, metallization coefficient, aspect ratio and duty factor of metal electrodes etc. This method has been already successfully applied to simulation of the Lamb wave characteristics in AlN/SiO<sub>2</sub> structures with improved temperature characteristics [6].

From the numerically found dependences  $f_R(s)$  and  $f_A(s)$ , which satisfy the electrical boundary conditions of the SC and OC gratings, respectively, the Lamb wave velocity dispersion was calculated,  $V_{R,A}(s)=pf_{R,A}(s)/s$ , where  $f_R$  and  $f_A$  are the resonant and anti-resonant frequencies. The electro-mechanical coupling coefficient  $k^2$  was estimated from the difference between  $V_R$  and  $V_A$  at  $s=0.5$  or another fixed  $s$ . Variation of the spectral frequency  $s$  in the first Brillouin zone, i.e. between 0 and 1, reveals the existence of multiple stopbands built by the interactions between the counter-propagating Lamb waves of different symmetry and order.

## III. NUMERICAL RESULTS AND DISCUSSION

The calculated velocities of the Lamb waves  $s_0$ ,  $a_0$  and few higher-order modes propagating in AlN plate with Al grating on the top ( $h_{Al}/2p=0.004$ ) and uniform Al electrode ( $h/2p=0.004$ ) at the bottom of AlN are shown in Fig. 1(a) as functions of the normalized AlN thickness  $h_{AlN}/2p$ . The synchronous resonance condition,  $s=0.5$  or  $\lambda=2p$ , is assumed.

Fig. 1(b) shows the electromechanical coupling  $k^2$  of the modes  $s_0$ ,  $a_0$  and  $qa_1$  (quasi-anti-symmetric mode) and reflection coefficient  $\kappa$  of the mode  $s_0$ . The latter changes sign at  $h/2p=0.18$ . The high values  $k^2 > 2\%$  have been obtained for the modes  $s_0$  and  $qs_1$  when  $h_{\text{AIN}}/2p < 0.5$  and  $h_{\text{AIN}}/2p < 0.3$ , respectively. For the mode  $a_0$  maximum coupling  $k^2=0.85\%$  was obtained at  $h_{\text{AIN}}/2p \approx 0.5$ .

To see the difference between symmetric and anti-symmetric Lamb waves of a different order, the motions, which follow propagation of Lamb waves under the grating, are visualized as contour plots of the displacement components and also as deformation of the AlN plate in the XZ plane. The instantaneous displacements in the sagittal plane,  $u_1$  and  $u_3$  (along the propagating direction and normal to it, respectively) were calculated via rigorous numerical solution of the field equations (modified version of the SDA-FEM-SDA software [7]). For example, Fig. 2 shows displacements for the  $s_0$  and  $a_0$  modes at  $h_{\text{AIN}}=p$  [Fig.2(a), (b)], for  $qs_1$  and  $qa_1$  modes at  $h_{\text{AIN}}=p/2$  [Fig.2(c),(d)], and for  $qs_2$  and  $qa_2$  modes at  $h_{\text{AIN}}=2p$  [Fig.2(e), (f)].

When  $h_{\text{AIN}}=p$ , the vertical displacement  $u_3$  dominates in the structure of the  $s_0$  and  $a_0$  modes [Fig. 2 (a, b)]. The waves are nearly perfect symmetric and anti-symmetric modes, with opposite or similar signs of  $u_3$  on the top and bottom surfaces of the AlN plate, respectively. A gradual decreasing of  $u_3$  from the top surface of the AlN plate, adjacent to the grating, towards the bottom surface can be observed in Fig. 2(b). This trend can be explained by the asymmetry of the analyzed structure with respect to the median plane,  $z=0$ , due to different boundary conditions at the top and bottom surfaces of the AlN.

The mode  $qs_1$  propagating at  $h_{\text{AIN}}=p/2$  with velocity  $V=20689$  m/s and the coupling  $k^2=2.30\%$  [Fig. 2(c)] resembles a combination of two modes with wavelengths  $\lambda_1=V/f$  and  $\lambda_2=V/2f$ . Based on the behavior of  $u_3$ , it can be classified as a quasi-symmetric mode, whereas the mode  $qa_1$  [Fig.2(d)], which is mostly longitudinally polarized, can be referred to quasi-anti-symmetric modes. Generally, higher-order Lamb waves reveal a complicated structure and can be referred to as symmetric or anti-symmetric modes only conventionally. This is also true for the second-order modes propagating at  $h_{\text{AIN}}=2p$  [Fig.2(e-f)].

The number of maxima and minima of the displacement fields within the plate thickness depends on the thickness and the order of the mode [1]. Two maxima of  $u_1$  and  $u_3$  can be observed along the Z-axis for the mode  $qs_2$  [Fig. 2(e)] but the distribution of  $u_1$  along the thickness looks irregular. The mode  $qa_2$  [Fig. 2(f)] is characterized by the nearly vanishing amplitude of  $u_1$  at the top and bottom surfaces. For thick plates, Lamb wave theory [1] predicts a focusing of Lamb wave displacements in the depth for higher-order modes, in contrast to the ‘‘skin-effect’’ expected for zero-order modes.

If the AlN thickness is sufficiently large, a plate supports several Lamb waves and can be utilized for building a multiple-mode resonator. Interactions between the modes are possible in the grating when forward and backward Lamb waves of the same or different order and symmetry propagate

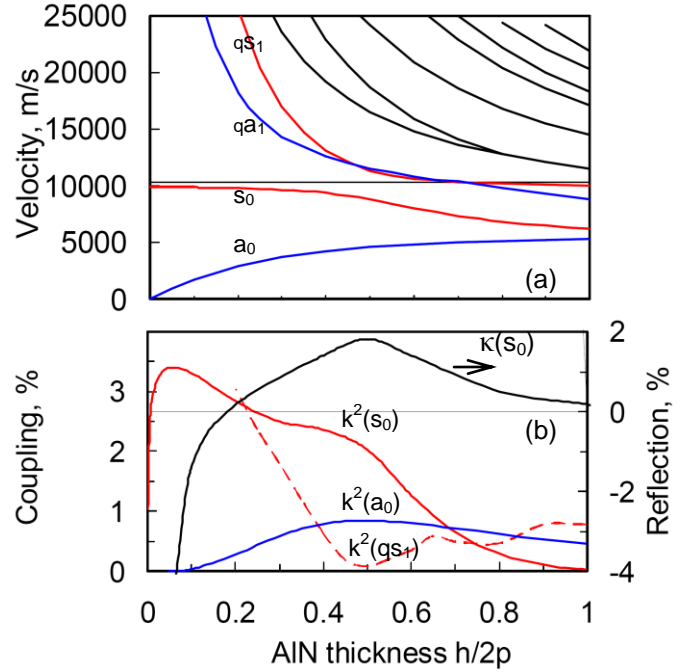


Fig. 1. Velocities of zero and higher-order Lamb waves propagating in SC Al grating (a), electromechanical coupling  $k^2$  of three Lamb waves and reflection coefficient  $\kappa$  of the mode  $s_0$  (b), as functions of AlN plate thickness in wavelengths  $\lambda=2p$ . The thickness of Al grating on top and Al electrode at the bottom is  $h_{\text{Al}}/\lambda=0.004$ .

with equal velocities. Such interactions can be predicted by simulation of the complete spectrum of modes existing in a resonator in a wide interval of spectral frequencies, from  $s=0$  to  $s=1$ , i.e. within the first Brillouin zone.

A combination of SDA-FEM-SDA technique with the Rational Approximation of harmonic admittance [8] was used to calculate the dispersion of Lamb waves under the grating. Fig.3 shows the simulated spectrum of Lamb waves in AlN resonators when  $h_{\text{AIN}}/2p$  varies between 0.1 and infinite thickness (AlN substrate). The normalized frequency  $f^*=fp/V_{\text{BAW}}=s \cdot V/V_{\text{BAW}}$ , where  $V_{\text{BAW}}=10287$  m/s is the longitudinal BAW velocity in AlN, stands for the variation of the spectral frequency  $s$  when the actual frequency  $f$  is fixed. Therefore, the dependencies  $V(f^*)$  shown in Fig.3 can be interpreted as the dispersion pattern  $\omega(k)$ , where  $k=2\pi f^*V_{\text{BAW}}/p/V(f^*)$  and  $\omega=V(f^*)/k$ . This pattern is a result of the interactions between the counter-propagating modes in the grating. If  $h_{\text{AIN}}/2p=0.1$  (Fig.3a), the modes  $a_0$  and  $s_0$  build the stopbands at  $f^*=0.08$  and  $f^*=(0.4-0.482)$  with the second resonance  $f_R(s_0)$  at the upper edge of the stopband because of the negative reflection coefficient  $\kappa$ . The velocities of  $a_0$  and  $s_0$  modes at resonance are 1683 and 9735 m/s, respectively, and  $k^2=3.3\%$  for  $s_0$  mode. Additional stopband is built by  $a_0/s_0$  interaction at  $f^*=0.17$  and  $\lambda \neq 2p$ . With  $h_{\text{AIN}}/2p$  increasing up to 0.5 (Fig. 3b), the frequency  $f_R(a_0)$  grows,  $f_R(s_0)$  decreases and shifts to the lower edge of the stopband ( $\kappa > 0$ ) whereas  $a_0/s_0$  interaction occurs at  $\lambda$  approaching  $2p$ . Finally, the symmetric, the anti-symmetric and the hybrid  $a_0/s_0$  modes merge into Rayleigh wave propagating along the surface of the AlN substrate (Fig. 3c).

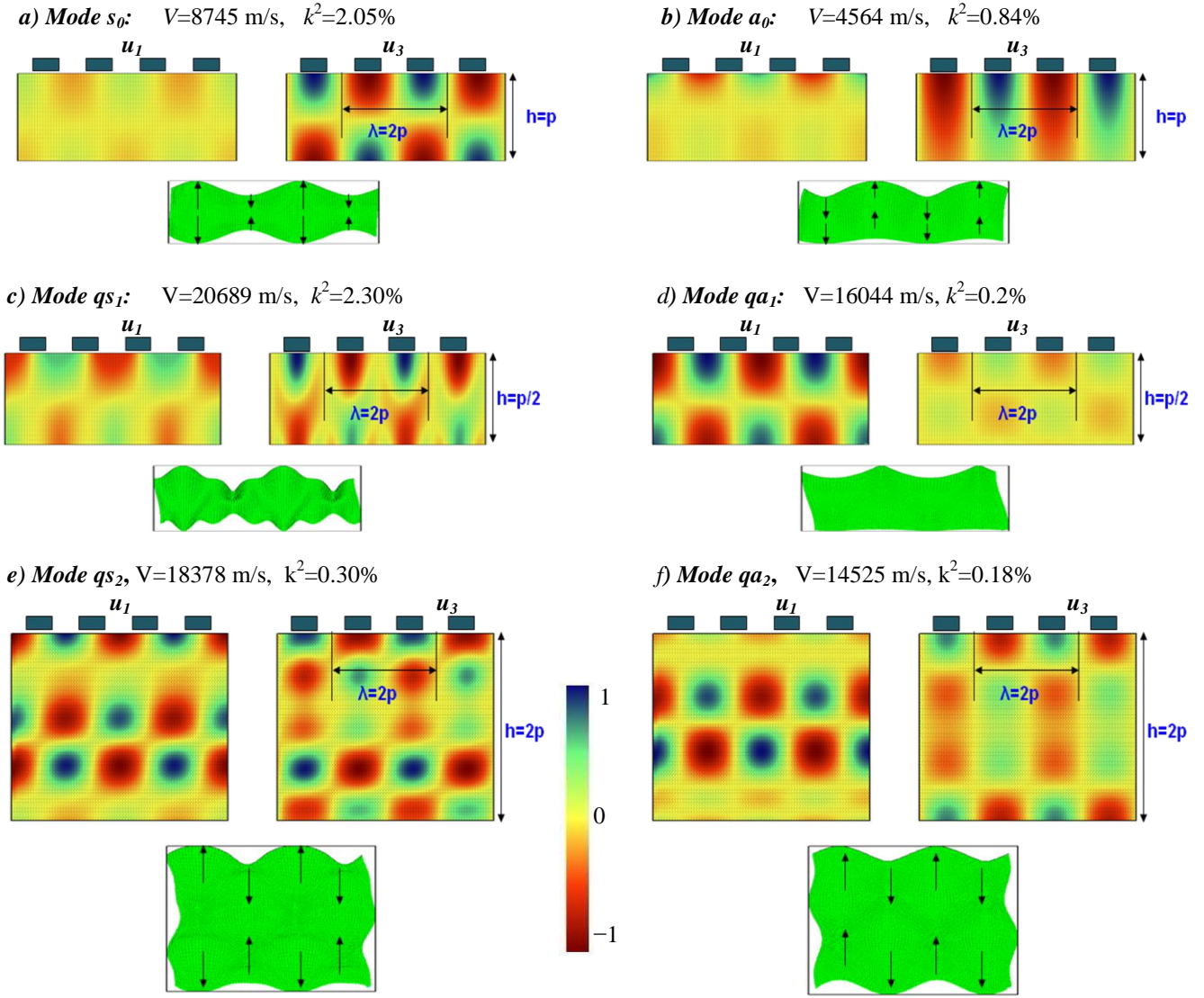


Fig. 2. Examples of Lamb wave structure in AlN plates of different thickness with SC grating: mode  $s_0$  (a) and  $a_0$  (b) when  $h=p$ ; higher-order quasi-symmetric (c) and quasi-anti-symmetric (d) modes in a plate of thickness  $h=p/2$ ; higher-order quasi-symmetric (e) and quasi-anti-symmetric (f) modes for plate thickness  $h=2p$ . Contour plots show instantaneous mechanical displacements  $u_1$  and  $u_3$  within four periods of the grating and along film thickness. Wave motions are schematically shown as perturbations of rectangular AlN plate.

Fig.4 shows the dispersion pattern obtained for  $h_{\text{AlN}}/2p=0.5$  as  $s(f)$  dependence, from which it is obvious that the stopband of the  $a_0$  and  $s_0$  modes occur at  $s=0.5$ , whereas the stopband built by  $a_0/s_0$  interaction refers to  $s\approx 1/3$  or  $\lambda\approx 3p$ . Another hybrid mode propagates in the grating when  $s\approx 1/4$  ( $\lambda\approx 4p$ ) and arises from the interaction between the  $qs_1$  and  $a_0$  modes.

Interactions between the counter-propagating Lamb waves of different order and symmetry can be approximately predicted from the analytical Lamb wave dispersion equations, ignoring the effect of a periodic grating. Such an interaction requires that  $k_1 + k_2 = 2k_0$ , where  $k_1$  and  $k_2$  are the wave numbers of the involved Lamb waves. For effective reflection of Lamb waves by the grating with a pitch  $p$ , it is desirable that  $\lambda=np$ , where  $n$  is a small integer. Then, the intermode coupling can occur at the frequency  $f$  if  $V_1(f)/V_2(f)=n-1$ , which requires  $V_1\approx 2V_2$  to obtain resonance at  $\lambda=3p$  and  $V_1\approx 3V_2$  for

resonance at  $\lambda=4p$ . From analytical dispersion equations, interaction between the modes  $a_0$  and  $s_0$  is possible at  $h_{\text{AlN}}f=2.9 \text{ MHz}\cdot\mu\text{m}$ , when  $V_{s_0}=9620 \text{ m/s}$  and  $V_{a_0}=4810 \text{ m/s}$ , e.g. when  $f=1 \text{ GHz}$ ,  $p=3.21 \mu\text{m}$  and  $h=2.9 \mu\text{m}$ . The numerical simulations with the SDA-FEM-SDA software, which consider the geometrical parameters of the analyzed Lamb wave resonator and perturbation of the modes by interactions between them, yield  $V=9614 \text{ m/s}$  and  $k^2=2.06\%$  for an AlN resonator with thickness  $h=0.8p$ , or a refined value of the thickness-frequency product  $h_{\text{AlN}}f=2.56 \text{ MHz}\cdot\mu\text{m}$ .

The structure of the analyzed hybrid mode is illustrated in Fig. 5. The wave is quasi-anti-symmetric mode with the wavelength  $\lambda=3p$ , though anti-symmetric mode  $a_0$  with velocity  $V_{a_0}\approx 4807 \text{ m/s}$  and twice smaller wavelength  $\lambda=1.5p$  dominates in the structure of the hybrid mode.

#### IV. CONCLUSIONS

Analysis of Lamb wave dispersion in a periodic grating with spectral frequency as parameter has revealed that zero- and higher-order modes interact with each other and build a complicated pattern in the 2D space of actual and spectral frequencies. Each interaction is permitted at a certain value of the product of plate thickness and frequency, which can be estimated from analytical dispersion equations and refined via numerical analysis for a grating with a specified geometry.

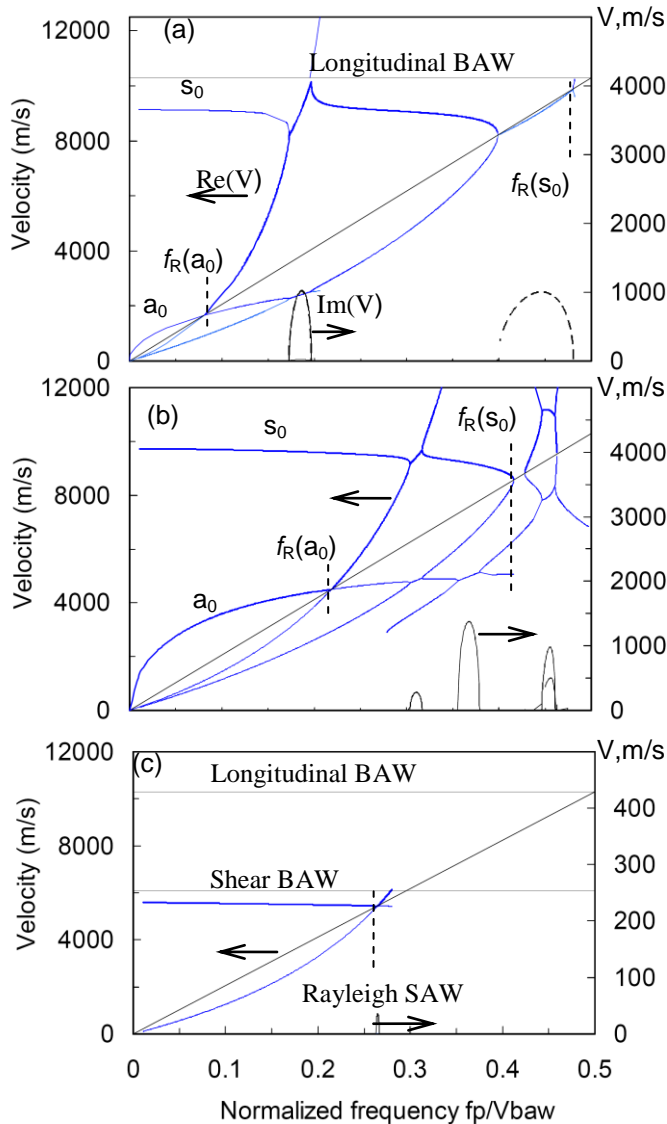


Fig. 3. Evolution of Lamb waves velocity dispersion when AlN plate thickness increases from  $h_{\text{AlN}}/2p=0.1$  (a) via  $h=p$  (b) to  $h_{\text{AlN}} \rightarrow \infty$  (AlN substrate) (c).

#### REFERENCES

[1] I. A. Viktorov, "Rayleigh and Lamb Waves: physical theory and applications", Plenum Press, New York, 1967  
 [2] V. Yanchev and I. Katardjiev, "Micromachined thin film plate acoustic wave mode", *IEEE Trans. Ultrason. Ferroelectr. Freq. Control*, vol.54, no 1, pp. 87-95, January 2007.  
 [3] J. H. Kuypers and A. P. Pisano, "Green Function Analysis of Lamb Wave Resonators", *Proc. 2008 IEEE Ultrasonics Symp.*, pp. 1548-1551.

[4] F. Di Pietrantonio, M. Benetti, D. Cannata, R. Beccherelli, and E. Verona, "Guided Lamb Wave Electroacoustic Devices on Micromachined AlN/Al Plates", *IEEE Trans. Ultrason. Ferroelectr. Freq. Control*, vol. 57, pp.1175-1182, May 2010.  
 [5] N. F. Naumenko, "A Universal Technique for Analysis of Acoustic Waves in Periodic Grating Sandwiched Between Multi-Layered Structures and Its Application to Different Types of Waves", *Proc. IEEE Ultrasonics Symp.*, pp. 1673-1676, 2010.  
 [6] N. F. Naumenko, "Temperature Compensated AlN/SiO<sub>2</sub> structures for Lamb Wave Resonators", *Proc. IEEE Ultrasonics Symp.*, Dresden, Oct.15-18, 2012, pp.795-798.  
 [7] N. F. Naumenko, and B. P. Abbott, "Transformation of Acoustic Waves in Periodic Metal Grating Sandwiched Between Piezoelectric and Dielectric", *IEEE Trans. UFFC*, 2011, vol. 58, no. 10, pp.2181-2187.  
 [8] N. F. Naumenko, and B. P. Abbott, "Fast Numerical Technique for Simulation of SAW Dispersion in Periodic Gratings and Its Application to Some SAW Materials", in *Proc. IEEE Ultrasonics Symp.*, New York, USA, Oct. 27-31, 2007, pp.166-170.

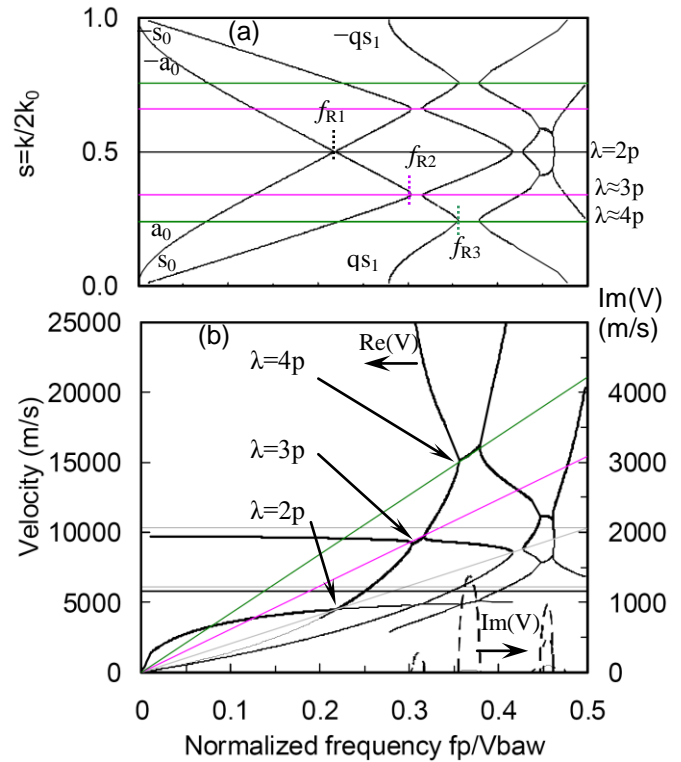


Fig.4. Perturbed wave numbers (a) and velocities (b) of the forward and backward propagating waves in AlN plate with SC grating, as functions of the normalized frequency. AlN thickness is  $h=p$ . Interactions between the modes  $a_0$ ,  $s_0$  and  $qs_1$  result in the stopbands and resonances at  $f_{R1}$ ,  $f_{R2}$  and  $f_{R3}$ .

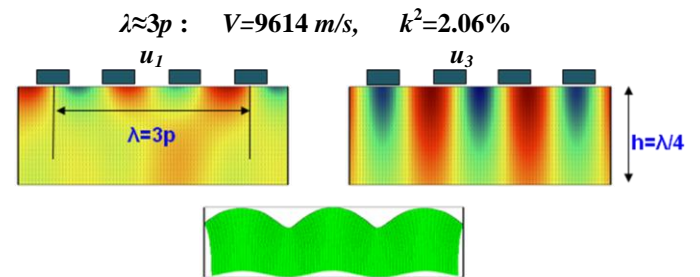


Fig. 5. Instantaneous mechanical displacements  $u_1$  and  $u_3$  and wave motions caused by the hybrid mode, which is built at  $\lambda=3p$  due to interaction between the counter-propagating  $a_0$  and  $s_0$  modes.